Published in final edited form as:
Mov Disord. 2011 August 1; 26(9): 1627–1632. doi:10.1002/mds.23643.

Combined R2* and diffusion tenser imaging changes in the substantia nigra in Parkinson disease

Guangwei Du, M.D., Ph.D.[1], **Mechelle M. Lewis, Ph.D.**[1,2], **Martin Styner, Ph.D.**[8,9], **Michele L. Shaffer, Ph.D.**[7], **Suman Sen, M.D.**[1], **Qing X. Yang, Ph.D.**[3,4,6], and **Xuemei Huang, M.D., Ph.D.**[1,2,3,4,5,6,10]

[1] Department of Neurology, Pennsylvania State University-Milton S. Hershey Medical Center, Hershey PA 17033

[2] Department of Pharmacology, Pennsylvania State University-Milton S. Hershey Medical Center, Hershey PA 17033

[3] Department of Radiology, Pennsylvania State University-Milton S. Hershey Medical Center, Hershey PA 17033

[4] Department of Neurosurgery, Pennsylvania State University-Milton S. Hershey Medical Center, Hershey PA 17033

[5] Department of Kinesiology, Pennsylvania State University-Milton S. Hershey Medical Center, Hershey PA 17033

[6] Department of Bioengineering, Pennsylvania State University-Milton S. Hershey Medical Center, Hershey PA 17033

[7] Department of Public Health Sciences, Pennsylvania State University-Milton S. Hershey Medical Center, Hershey PA 17033

[8] Department of Computer Science, University of North Carolina, Chapel Hill, NC 27599

[9] Department of Psychiatry, University of North Carolina, Chapel Hill, NC 27599

[10] Department of Neurology, University of North Carolina, Chapel Hill, NC 27599

Abstract

Background—Recent magnetic resonance imaging (MRI) studies suggest increased transverse relaxation rate (R2*) and reduced diffusion tensor imaging (DTI) fractional anisotropy (FA) values in the SN in PD. The R2* and FA changes may reflect different aspects of PD-related

Corresponding Author: Xuemei Huang MD, PhD, Associate Professor of Neurology, Penn State Hershey Medical Center, 500 University Dr., H-037, Hershey, PA 17033-0850, Voice: 717-531-1530 Fax: 717-531-0226, xuemei@psu.edu.

Author Roles:
1. Research project: A. Conception, B. Organization, C. Execution;
2. Statistical Analysis: A. Design, B. Execution, C. Review and Critique;
3. Manuscript: A. Writing of the first draft, B. Review and Critique;
Guangwei Du: 1A, 1B, 1C, 2A, 2B, 3A.
Mechelle M. Lewis: 1B, 1C, 3A, 3B.
Martin Styner: 1A, 1B, 3B.
Michele L. Shaffer: 2A, 2C, 3B.
Suman Sen: 1B, 1C, 3B.
Qing Yang: 1A, 1B, 3B.
Xuemei Huang: 1A, 1B, 1C, 2A, 2C, 3B.

Full Financial Disclosures of all Authors for the Past Year: The authors have reported no disclosures.

Financial Disclosure: The authors have reported no disclosures.

pathological processes (i.e., tissue iron deposition and microstructure disorganization). This study investigated the combined changes of R2* and FA in the SN in PD.

Methods—High resolution MRI (T2-weighted, T2*, and DTI) were obtained from 16 PD and 16 Controls. Bilateral SNs were delineated manually on T2-weighted images and co-registered to R2* and FA maps. The mean R2* and FA values in each SN then were calculated and compared between PD and Controls. Logistic regression, followed by ROC curve analysis, was employed to investigate the sensitivity and specificity of the combined measures for differentiating PD subjects from Controls.

Results—Compared to Controls, PD subjects demonstrated increased R2* ($p<0.0001$) and reduced FA ($p=0.0365$) in the SN. There was no significant correlation between R2* and FA values. Logistic regression analyses indicated that the combined use of R2* and FA values provides excellent discrimination between PD and Controls (c-statistic=0.996) compared to R2* (c-statistic=0.930) or FA (c-statistic=0.742) alone.

Conclusions—This study shows that the combined use of R2* and FA measures in the SN of PD enhances the sensitivity and specificity in differentiating PD from Controls. Further studies are warranted to evaluate the pathophysiological correlations of these MRI measurements, and their effectiveness in assisting in diagnosing PD and following its progression.

Keywords

Parkinson's disease (PD); substantia nigra; diffusion tensor imaging (DTI); transverse relaxation rate (R2*); magnetic resonance imaging (MRI)

Introduction

Parkinson's disease (PD) is marked pathologically by the loss of dopaminergic neurons in the substantia nigra (SN) of the basal ganglia. Both the understanding of the pathogenesis of PD-associated cell loss and evaluation of potential neuroprotective therapies have been hindered by the lack of a reliable, objective, easily obtainable, *in vivo* marker(s) for disease diagnosis and progression. Advances in magnetic resonance imaging (MRI) have begun to allow interrogation of ongoing pathological processes in PD with quantitative parametric mapping methods.[1–4]

Both cell and animal data suggest a role for iron in PD pathoetiology, including increased iron content in the SN of PD subjects.[5–7] Trivalent iron (Fe^{3+}) is paramagnetic and causes a strong reduction in T2* relaxation time. Several MRI studies have shown that R2*(1/T2*) in the SN is correlated with iron concentration *in vivo*[8–10], and is increased in PD.[1,2,11–13] In addition, neurodegenerative processes may lead to a disruption of microstructural integrity (e.g., cell death and associated changes in myelinated processes of fibers *en passant*). The altered local diffusion characteristics of water molecules in the corresponding brain region then can be quantified by diffusion tensor imaging (DTI).[14,15] DTI changes have been correlated with loss of SN dopamine neurons in mice treated with 1-methyl-4-phenyl-1,2,3,6-tetrahydropyridine (MPTP),[16] and recent studies in PD patients demonstrated reduced fractional anisotropy (FA) in the SN.[3,4,13,17]

R2* and FA changes may reflect different aspects of PD-related pathological processes (i.e., tissue iron deposition and microstructure disorganization). This study was designed to investigate the changes of both R2* and FA in the SN in PD and the potential of using their combined measurements to discriminate PD subjects from Controls.

Methods

Subjects

Sixteen PD and 16 control subjects matched in age and gender distribution were recruited from a tertiary movement disorders clinic (see Table 1 for detailed demographic information). PD diagnosis was confirmed by a movement disorder specialist (XH) according to published criteria.[18] Unified Parkinson's Disease Rating Scale part III motor scores (UPDRS-III) were obtained for each PD subject after withholding all PD medication overnight (~12 hr). All subjects gave written informed consent, consistent with the Declaration of Helsinki and reviewed and approved by the Penn State University Institutional Review Board.

Data acquisition

All subjects were scanned with a 3.0 Tesla MR Scanner (Trio, Siemens Magnetom, Erlangen, Germany, with an 8-channel phased array head coil) with high-resolution T2-weighted images, multi-echo susceptibility weighted images (SWI), and diffusion tensor images (DTI). A fast-spin-echo sequence was used to obtain T2-weighted images with TR/TE = 2500/316, FOV = 256 mm × 256 mm, matrix = 256 × 256, slice thickness = 1 mm (with no gap), slice number = 176. A multi-echo SWI sequence was used to estimate the proton transverse relaxation rate, R2* (R2* = 1/T2*). Six echoes with TE ranging from 7 to 47 ms and an interval of 8 ms were acquired with TR = 54 ms, flip angle = 20°, FoV = 256 mm × 256 mm, matrix = 256 × 256, slice thickness = 1 mm (with no gap), slice number = 64. The middle slice of the SWI was placed on the line between the anterior and posterior commissures. For DTI, acquisition parameters were as follows: TR/TE = 8300/82 ms, b value = 0, 1000 s/mm^2, diffusion gradient directions = 42, FoV = 256 mm × 256 mm, matrix = 128 × 128, slice thickness = 2 mm (with no gap), slice number = 65.

Image processing and analysis

Generation of R2* and DTI maps—The magnitude images of multi-echo SWI images were used to generate R2* maps by using a voxel-wise linear least-squares fit to a mono-exponential function with free baseline using an in-house MATLAB (The MathWorks, Inc., Natick, MA) tool. For DTI images, the distortions induced by eddy currents and head motion first were corrected by affine registration of all diffusion-weighted images to the first B0 image for each subject.[19] FA, mean diffusivity (MD), axial diffusivity (AD), and radial diffusivity (RD) maps then were generated by using FMRIB's Diffusion Toolbox (www.fmrib.ox.ac.uk/fsl).[20]

Segmentation of substantia nigra—A two-step semiautomatic strategy to obtain R2* and DTI measures in the SN was developed to minimize the subjectivity of MRI data analysis. First, bilateral SN were manually segmented on multi-slice high resolution T2-weighted images by an investigator blinded to the diagnosis of each subject according to previously described methods[2,21] using ITK-SNAP (www.itksnap.org).[22] The SN was defined as a hypointensity band between the red nucleus and cerebral peduncle in axial sections as illustrated in Figure 1A. To minimize the possibility of including the subthalamic nucleus, the segmentation of the SN was started either at the level of the red nucleus showing the largest radius, or one slice lower, depending on the slice in which the SN appeared most prominently. Despite this best effort, it is still possible that a small portion of the subthalamic nucleus was included in the anterior dorsal part of our segmentation. Then, a total of 6–8 slices (dorsal to ventral, ~6–8 mm height) were used to define the SN. Second, the segmented bilateral SNs were mapped to R2* and FA maps as shown in Figures 1B and 1C, respectively, by co-registering the T2-weighted images to R2*maps and the B0 images of DTI data using an affine registration pipeline implemented in 3D Slicer (www.slicer.org).

R2* values in the SN of each subject were calculated using trimmed means (from the 5%–95% percentile) to reduce variability introduced by manual segmentation and imperfect registration processes. The trimmed means were used here because they represent a more robust central estimator of the measurement, and they are based on the assumption that the top and bottom values represent extreme measures (potential outliers). As the SN is a heterogeneous structure containing axons, nuclei, and blood vessels, in addition to having decreased spatial resolution (2 × 2 × 2 mm) compared to other imaging sequences, DTI data sets (FA, MD, AD, and RD values) are expected to be highly variable. In order to compensate for this intrinsically high variance in DTI measurements, a narrower trimmed mean threshold (from the 25%–75% percentile) was employed.

Statistical Analysis

PD and Control demographics were compared using two-sample t-tests and Fisher's exact tests as appropriate. The association between R2* and DTI measures was quantified via Pearson correlation. Regional R2* and DTI values were compared separately between PD and control subjects by analyses of covariance with adjustments for age and gender. The relationship between UPDRS-III scores, disease duration, and MRI measurements were explored by simple linear regression. Logistic regression and receiver operating characteristic (ROC) curves were used to compare the sensitivity and specificity separately for R2* and FA and for their combination. The c-statistic, representing the area under the ROC curve, was calculated as a measure of discrimination. All statistical analyses were performed using SAS 9.2 (SAS Institute Inc., Cary, NC, USA).

Results

The demographic and clinical data are summarized in Table 1. There were no significant differences between PD and control subjects in age or gender. *Compared to the bilateral mean of control subjects,* PD subjects had significant increases in the bilateral mean of R2* values in the SN [p<0.0001] (Figure 2). This significant difference remained strong when comparing the SN either contralateral or ipsilateral to the most affected limb in PD [p<0.0001]. *Compared to the bilateral mean of control subjects,* PD subjects had significantly reduced FA values in the bilateral mean of FA values in the SN [p=0.0365]. Interestingly, these significant differences in the FA values seemed to be more pronounced in the SN contralateral to the more affected limb [p=0.0427] than in the SN ipsilateral to the more affected limb [p=0.0947] (Figure 2). In addition to FA values, an increased but not statistically significant RD value was found in the bilateral mean [p=0.0578] in the SN. There were no significant differences in MD or AD between PD and control subjects. In addition, there were no significant correlations between either UPDRS-III scores and MRI measures (R2*: [r^2=0.2686, p=0.3145], FA: [r^2=−0.0297, p=0.9132]) or disease duration and MRI measures (R2*: [r^2=−0.0713, p=0.9747], FA: [r^2=0.1119, p=0.2053]) in the SN of PD subjects.

As shown in the scatter plot of bilateral R2* and FA values (Figure 3A), there was no significant trend or correlation between R2* and FA values in the SN in the overall study group (PD and Controls), or between R2* and MD, AD, or RD (data not shown). The individual Pearson correlation coefficient of bilateral R2* and FA values in PD subjects was −0·3491 (p=0.2022) and in control subjects 0.1160 (p=0.6805). The most striking feature revealed by this plot, however, is the clear separation between the two groups. Evidently, collapsing any one of the two dimensions would result in overlapping of the one group by the other.

The results of the logistic regression models predicting PD status from either R2* or FA alone or in combination are shown in Table 2. The odds of PD are quintupled for each half

standard deviation increase in R2* when using R2* alone, and the odds of PD are more than halved for each half standard deviation increase in FA when using FA alone. When using the combination of R2* and FA, the odds of PD are quadrupled for each half standard deviation increase in R2* holding FA constant, whereas the odds of PD are quartered for each half standard deviation increase in FA, holding R2* constant. The ROC curves displayed in Figure 3B show that the combined R2* and FA ROC curve lies above both the R2* alone and FA alone ROC curves, illustrating the increased sensitivity and specificity of the combined measures. There was significant discrimination between the groups using either R2* or FA alone (R2*: c-statistic=0.930; p-value<0.0001; FA: c-statistic=0.742 p-value<0.0001). The combination of R2* and FA in the SN, however, yielded an even greater discrimination (c-statistic=0.996; p-value<0.0001).

Discussion

There are three main results from this study. First, PD subjects show both significantly increased R2* and reduced FA values in the SN compared to Controls. Second, there is no significant correlation between these two MRI measurements, suggesting that R2* and FA changes may reflect different pathological aspects of PD occurring in the SN. Third, whereas R2* and FA can discriminate PD subjects and Controls, combined they appear to discriminate both sensitively and specifically between these two groups. Further studies are warranted to evaluate the pathophysiological correlations of these MRI measurements, and their effectiveness in assisting in diagnosing PD and following its progression.

Our findings of a significant increase in R2* and decrease in FA values in PD compared to Controls are consistent with previous reports.[1–4,13] In all previous studies, however, the SN was defined on the parametric maps that were subsequently used to determine the R2* or FA values. This is not only technically challenging, but also may be susceptible to rater bias when unblinded drawing is performed. In our study, we simplified the procedure and minimized the rater bias by implementing a two-step, semi-automated approach. In the first step (manual delineation of the SN), we chose an MRI sequence (T2-weighted) that is conventional and accepted by radiologists for use in defining the SN.[9,21] In the second step (determining the R2* and FA values themselves), we co-registered the pre-defined region of interest (ROI) to R2* and FA maps and calculated the means automatically. Identification of the SN in T2-weighted images, however, is difficult partially because of the unclear boundary between the subthalamic nucleus and the SN. This is particularly problematic in the dorsal region of the SN.[23] In order to minimize inclusion of the subthalamic nucleus, we chose to begin segmentation of the SN at the axial level where the SN appears prominently. Despite our best efforts, it is still possible that the SN defined in the current study may include some small portion of the subthalamic nucleus.

Unlike the previous study by Martin et al.,[1] we did not find a significant correlation between R2* in the SN and UPDRS motor scores in PD subjects. This discrepancy may be due to the fact that we did not separate the SN into its pars compacta (SNc) and pars reticulata (SNr) subregions. Even with the improved resolution of a 3T scanner, defining the border between SNc and SNr in T2-weighted images has been difficult and remains controversial.[21] In addition, the parameters for our DTI sequences only allowed a spatial resolution of $2 \times 2 \times 2$ mm^3, inadequate for delineating these SN subregions. Future research and additional tools are needed to develop an objective method for separation of the SNc and SNr in order to understand the region-specific relationships between iron deposition in the SN and PD symptomatology, which is not addressed in this paper.

We did not find a significant correlation between FA values in the SN and UPDRS motor scores in PD, consistent with previous work by Vaillancourt et al.[4] Interestingly, the

decrease in FA values in PD in the current study appeared to be more robust on the side contralateral to the more symptomatic side. This result hints that FA values may have utility in reflecting disease severity, although further studies with larger sample sizes are needed to test this hypothesis. Moreover, the most important finding in the previous work by Vaillancourt et al. was the demonstration of a dopamine cell loss pattern in the SN using DTI that is consistent with earlier immunohistochemistry studies[4,24]. Higher spatial resolution imaging and improved ROI definition protocols should be developed to study the imaging characteristics in different SN segments.

Compared with recent work by Peran et al.,[13] the current study focused on the SN and two parametric measures of MRI (R2* and FA) rather than including additional basal ganglia nuclei, and thalamus, along with morphometric measurements. In addition, whereas Peran et al. [13] reported hemisphere-specific measures (right or left), our study presented the R2* and FA values relative to the more and less affected side in PD. Although we did not find significant correlations between either FA or R2* and the clinical scores, this may be hampered by our limited sample size. We also did not include morphometric information for the SN since the boundary of the SN seen in T2-weighted images is imperfect, and the current manual delineation approach for the SN does not yield a reliable volumetric measurement.

Although R2* is known to reflect iron concentration[10] and FA measures local diffusion characteristics of water molecules,[14,15] the exact pathophysiological meaning of the changes in these measurements in PD are unknown. The data from the current study suggest that R2* and FA are correlated neither in PD nor Controls, supporting the hypothesis that these two MRI measurements may reflect different aspects of PD-related pathological and/or etiological changes in the SN. Further basic scientific and clinical studies are warranted to understand the pathophysiological correlations of these *in vivo* MRI measures in PD.

In this study, the combination of R2* and FA measures improved the overall discrimination between PD and Controls, providing a high degree of sensitivity and specificity, with close to perfect discrimination of PD subjects from Controls as evidenced by the ROC curves. This raises several interesting possibilities that we feel deserve consideration by the field as a whole. First, will this combination imaging approach allow for unbiased monitoring of disease progression? Second, can these MRI changes be seen early in the disease or even premorbidly? Third, will this approach be adequately sensitive and specific to discriminate PD either from other parkinsonisms (e.g., multiple system atrophy and progressive supranuclear palsy), or from other neurodegenerative disorders? Whatever the answer to these questions, the current study offers the possibility of using the combined MRI measures as a non-invasive, practical tool for the diagnosis of PD and monitoring its progression.

Acknowledgments

This work was supported by NS060722 (GD, MML, QXY, and XH), and the HMC GCRC (NIH M01RR10732) and GCRC Construction Grant (C06RR016499). We also would like to thank all the participants in the study, as well as the support of the study coordinator Ms. Eleanore Hernandez and MRI technical support from Dr. Jianli Wang and Mr. Jeffery Vesek. We also would like to thank Dr. Richard Mailman for his helpful comments on the manuscript.

References

1. Martin WR, Wieler M, Gee M. Midbrain iron content in early Parkinson disease: a potential biomarker of disease status. Neurology. 2008; 70(16 Pt 2):1411–1417. [PubMed: 18172063]

2. Gorell JM, Ordidge RJ, Brown GG, Deniau JC, Buderer NM, Helpern JA. Increased iron-related MRI contrast in the substantia nigra in Parkinson's disease. Neurology. 1995; 45(6):1138–1143. [PubMed: 7783878]
3. Chan LL, Rumpel H, Yap K, Lee E, Loo HV, Ho GL, et al. Case control study of diffusion tensor imaging in Parkinson's disease. J Neurol Neurosurg Psychiatry. 2007; 78(12):1383–1386. [PubMed: 17615165]
4. Vaillancourt DE, Spraker MB, Prodoehl J, Abraham I, Corcos DM, Zhou XJ, et al. High-resolution diffusion tensor imaging in the substantia nigra of de novo Parkinson disease. Neurology. 2009; 72(16):1378–1384. [PubMed: 19129507]
5. Earle KM. Studies on Parkinson's disease including x-ray fluorescent spectroscopy of formalin fixed brain tissue. J Neuropathol Exp Neurol. 1968; 27(1):1–14. [PubMed: 5656584]
6. Dexter DT, Wells FR, Lees AJ, Agid F, Agid Y, Jenner P, et al. Increased nigral iron content and alterations in other metal ions occurring in brain in Parkinson's disease. J Neurochem. 1989; 52(6): 1830–1836. [PubMed: 2723638]
7. Sofic E, Riederer P, Heinsen H, Beckmann H, Reynolds GP, Hebenstreit G, et al. Increased iron (III) and total iron content in post mortem substantia nigra of parkinsonian brain. J Neural Transm. 1988; 74(3):199–205. [PubMed: 3210014]
8. Ordidge RJ, Gorell JM, Deniau JC, Knight RA, Helpern JA. Assessment of relative brain iron concentrations using T2-weighted and T2*-weighted MRI at 3 Tesla. Magn Reson Med. 1994; 32(3):335–341. [PubMed: 7984066]
9. Gelman N, Gorell JM, Barker PB, Savage RM, Spickler EM, Windham JP, et al. MR imaging of human brain at 3.0 T: preliminary report on transverse relaxation rates and relation to estimated iron content. Radiology. 1999; 210(3):759–767. [PubMed: 10207479]
10. Haacke EM, Cheng NY, House MJ, Liu Q, Neelavalli J, Ogg RJ, et al. Imaging iron stores in the brain using magnetic resonance imaging. Magn Reson Imaging. 2005; 23(1):1–25. [PubMed: 15733784]
11. Ye FQ, Allen PS, Martin WR. Basal ganglia iron content in Parkinson's disease measured with magnetic resonance. Mov Disord. 1996; 11(3):243–249. [PubMed: 8723139]
12. Baudrexel S, Nurnberger L, Rub U, Seifried C, Klein JC, Deller T, et al. Quantitative mapping of T1 and T2* discloses nigral and brainstem pathology in early Parkinson's disease. Neuroimage. 2010
13. Peran P, Cherubini A, Assogna F, Piras F, Quattrocchi C, Peppe A, et al. Magnetic resonance imaging markers of Parkinson's disease nigrostriatal signature. Brain. 2010
14. Basser PJ, Pierpaoli C. Microstructural and physiological features of tissues elucidated by quantitative-diffusion-tensor MRI. J Magn Reson B. 1996; 111(3):209–219. [PubMed: 8661285]
15. Mori S, Zhang J. Principles of diffusion tensor imaging and its applications to basic neuroscience research. Neuron. 2006; 51(5):527–539. [PubMed: 16950152]
16. Boska MD, Hasan KM, Kibuule D, Banerjee R, McIntyre E, Nelson JA, et al. Quantitative diffusion tensor imaging detects dopaminergic neuronal degeneration in a murine model of Parkinson's disease. Neurobiol Dis. 2007; 26(3):590–596. [PubMed: 17428671]
17. Yoshikawa K, Nakata Y, Yamada K, Nakagawa M. Early pathological changes in the parkinsonian brain demonstrated by diffusion tensor MRI. J Neurol Neurosurg Psychiatry. 2004; 75(3):481–484. [PubMed: 14966170]
18. Calne DB, Snow BJ, Lee C. Criteria for diagnosing Parkinson's disease. Ann Neurol. 1992; 32 (Suppl):S125–S127. [PubMed: 1510370]
19. Jenkinson M, Smith S. A global optimisation method for robust affine registration of brain images. Med Image Anal. 2001; 5(2):143–156. [PubMed: 11516708]
20. Smith SM, Jenkinson M, Woolrich MW, Beckmann CF, Behrens TE, Johansen-Berg H, et al. Advances in functional and structural MR image analysis and implementation as FSL. Neuroimage. 2004; 23 (Suppl 1):S208–S219. [PubMed: 15501092]
21. Oikawa H, Sasaki M, Tamakawa Y, Ehara S, Tohyama K. The substantia nigra in Parkinson disease: proton density-weighted spin-echo and fast short inversion time inversion-recovery MR findings. AJNR Am J Neuroradiol. 2002; 23(10):1747–1756. [PubMed: 12427635]

22. Yushkevich PA, Piven J, Hazlett HC, Smith RG, Ho S, Gee JC, et al. User-guided 3D active contour segmentation of anatomical structures: significantly improved efficiency and reliability. Neuroimage. 2006; 31(3):1116–1128. [PubMed: 16545965]

23. Vaillancourt DE, Spraker MB, Prodoehl J, Zhou XJ, Little DM. Effects of aging on the ventral and dorsal substantia nigra using diffusion tensor imaging. Neurobiol Aging. 2010

24. Fearnley JM, Lees AJ. Ageing and Parkinson's disease: substantia nigra regional selectivity. Brain. 1991; 114 (Pt 5):2283–2301. [PubMed: 1933245]

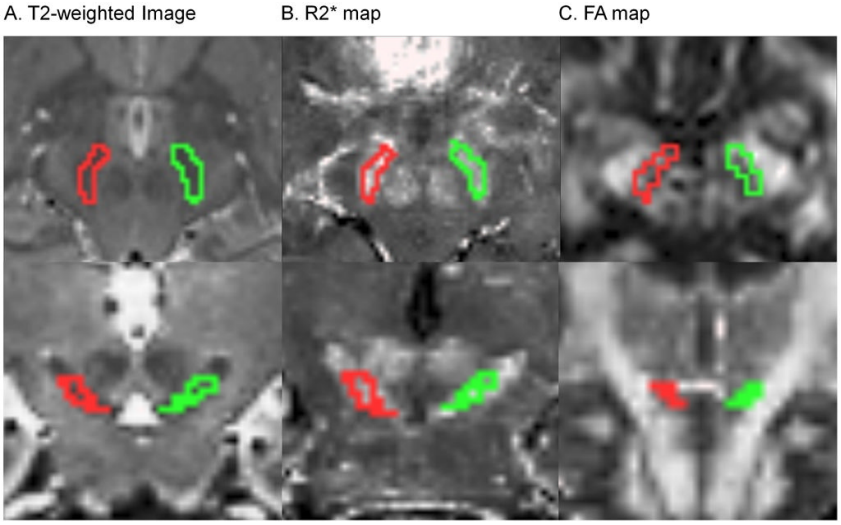

Figure 1.
A typical image illustrated the location of the substantia nigra in T2-weighted images (A) and the co-registered ROIs on the R2* (B) and FA (C) maps on both axial (top row) and coronal (bottom row) sections.

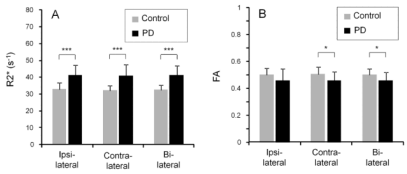

Figure 2. Comparison of R2* and FA values in PD and Controls

Comparison of R2* (A) and FA (B) values between PD and control subjects in ipsilateral, contralateral, and bilateral SN. Gray bars represent control subjects and black bars represent PD subjects. Signficant differences between PD and control subjects are represented as: *: $p<0.05$; ***: $p<0.001$.

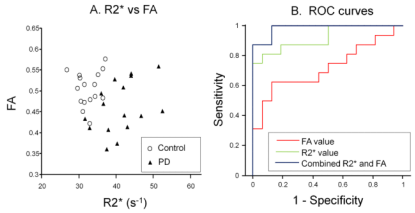

Figure 3. Correlation of R2* and FA, along with ROC curves

A is the scatter plot of bilateral R2* and FA. B represents the ROC curves for discrminating between PD and control subjects generated by using FA (red line), R2* (green line), or their combination (dark blue line).

Table 1

Demographics for control and Parkinson's subjects

	Controls	PD	p-value*
No. (female, male)	16 (9, 7)	16 (7, 9)	0.724
Age, years (mean ± SD)	57.2 ± 6.8	59.2 ± 6.9	0.407
UPDRS-III motor score (mean ± SD)	-	23.1 ± 12.3	-
Disease duration, year (mean ± SD)	-	4.8 ± 3.0	-

* p-value is based on Fisher's exact test for gender and two-tailed, two-sample t-test for age.

Table 2

Logistic regression results for predicting PD status from R2* or FA alone or in combination

		Odds Ratio* (95% Confidence Interval)	p-value	c-statistic	Goodness-of-fit (Hosmer & Lemeshow) p-value
Model (R2*)		5.038 (1.357, 18.710)	0.016	0.930	0.827
Model (FA)		0.635 (0.411, 0.983)	0.041	0.742	0.354
Model (R2* + FA)	R2*	8.682 (1.212, 62.204)	0.031	0.996	0.956
	FA	0.180 (0.029, 1.110)	0.065		

*Expressed as a half standard deviation increment